Retinotopic mapping in awake monkeys suggests a different functional organization for dorsal and ventral V4

Denis Fize, Wim Vanduffel, Koen Nelissen, Katrien Denys, Christophe Chef d'Hotel, Olivier Faugeras, Guy A. Orban

INSTITUT DE RECHERCHE EN INFORMATIQUE ET AUTOMATIQUE

Retinotopic mapping in awake monkeys suggests a different functional organization for dorsal and ventral V4

Denis Fize, Wim Vanduffel, Koen Nelissen, Katrien Denys, Christophe Chef d'Hotel, Olivier Faugeras and Guy A Orban

N° 4732
February, 2003

THEME 3

ISSN 0249-6399

Retinotopic mapping in awake monkeys suggests a different functional organization for dorsal and ventral V4

Denis Fize[1], Wim Vanduffel[1,2,#], Koen Nelissen[1], Katrien Denys[1], Christophe Chef d'Hotel[3], Olivier Faugeras[3] and Guy A Orban[1]

Thème 3 : Interaction homme-machine, images données, connaissances

Projet Odyssée

Rapport de Recherche n° 4732 – February, 2003 - 30 pages

Abstract: Using functional magnetic resonance imaging, we mapped the retinotopic organization throughout the visual cortex of fixating monkeys. The observed retinotopy in V1, V2 and V3 was completely consistent with the classical view. More rostrally in occipital cortex, both areas V3A and MT/V5 had a lower and upper visual field representation split by a horizontal meridian. Both areas were almost completely surrounded by a vertical meridian representation. Ventral, but not dorsal V4 was rostrally bordered by a horizontal meridian. Furthermore, contrary to all other early visual areas including V4v, the eccentricity lines ran almost parallel to the areal boundaries in V4d. These results suggest a different functional organization in dorsal and ventral V4, similar to what has been observed in humans.

Keywords: fMRI, Retinotopy, Visual Cortex

[1]Laboratorium voor Neuro- en Psychofysiologie Katholieke Universiteit Leuven, Campus Gasthuisberg Herestraat 49, Leuven B-3000, Belgium.

[2]MGH/MIT/HMS Athinoula A. Martino's Center for Biomedical Imaging 13th Street, Bldg 149, Charlestown, Massachusetts 02129, USA.

[3]Equipe Odyssée INRIA, UR de Sophia-Antipolis 2004 route des lucioles BP93
06902 Sophia-Antipolis Cedex France

La délinéation des aires visuelles rétinotopiques chez le singe éveillé suggère une organisation différente pour les parties dorsales et ventrales de V4

Résumé : Grâce à l'imagerie par résonance magnétique fonctionnelle, nous avons cartographié l'organisation rétinotopique du cortex visuel chez des singes éveillés. Les résultats de nos mesures dans V1, V2 et V3 sont tout à fait compatibles avec les connaissances actuelles. Dans des zones plus rostrales du cortex occipital, nous avons observé que les zones V3A et MT/V5 possédaient une représentation du champ visuel supérieur et inférieur séparées par une représentation du méridien horizontal. Les deux aires sont presque complètement entourées par une représentation du méridien vertical. La partie ventrale, mais pas dorsale, de V4, est bordée par une représentation du méridien horizontal. De plus, contrairement à toutes les autres aires visuelles, y compris V4v, les lignes d'eccentricité sont presque parallèles aux frontières de l'aire V4d. Ces résultats suggèrent une organisation fonctionnelle différente dans les parties dorsales et ventrales de V4, semblable à ce qui a été observé chez l'humain.

Mots-clés : IRMf, Rétinotopie, Cortex visuel

INTRODUCTION

Typically, visual cortical areas in the macaque can be identified based upon differences in anatomical connections, cyto- and myeloarchitecture, functional properties and retinotopic organization. Using a combination of these four criteria, monkey visual cortex has been tentatively parcellated into more than 30 different visual areas (Felleman and Van Essen, 1991). However, although borders of early visual areas are well-established (Daniel and Whitteridge, 1961; Van Essen et al., 1984), this has proven to be more complex in extrastriate cortex (see Van Essen, 2002, for review). The disagreement about *the* map starts as early as area V3, as it is still debated whether or not, a ventral counterpart of V3d exists in a region anterior to ventral V2 (Zeki, 1978; Burkhalter and Van Essen, 1986; Stepniewska and Kaas, 1996; Lyon and Kaas, 2002). In fact, area MT/V5 is the only higher tier area beyond V2 for which there is general agreement about its location and borders. Indeed, alternative division schemes have been proposed for area V4 (e.g. 'DL' and 'DM', by Kaas and colleagues), as well as the complete extent of the inferotemporal cortex (Ungerleider vs Van Essen schemes, see Van Essen et al., 2002), and the posterior parietal cortex (Seltzer and Pandya, 1978; Pandya and Seltzer, 1982; Colby et al., 1988; Andersen et al., 1990; Boussaoud et al., 1990; Felleman and Van Essen, 1991; Preuss and Goldman-Rakic, 1991; Lewis and Van Essen, 2000).

Several factors hamper a straightforward delineation of extrastriate visual areas. Firstly, detailed information about many extrastriate visual areas is lacking, simply because they have not been fully explored. For example, experimental studies of V4 usually concentrate on its easy-accessible dorsal subdivision, while its ventral portion remained largely unexplored territory. Secondly, as to now it is unclear whether clear-cut areal boundaries exist in far extrastriate cortex. It could be that at higher levels in the visual system functional and anatomical properties change more gradually from the one area to the next as compared to the abrupt transitions in early visual areas (less than 1 mm, e.g. Orban et al., 1980). Thirdly, to create *general* maps of well-explored areas it has been inevitable to extrapolate data acquired during a large number of invasive experiments performed in many different laboratories. By definition, this added a significant amount of variance to the 'mean' maps (see Van Essen et al., 2001). Therefore, to resolve most of the discrepancies between the existing maps, it would be necessary to perform large-scale invasive experiments in single subjects, an unrealistic prospect with the currently available technology.

The development of non-invasive functional imaging techniques during the past decade allowed to map the functional organization of human visual cortex (Engel et al., 1994; Sereno et al., 1995; DeYoe et al., 1996; Engel et al., 1997; Hadjikhani et al., 1998; Goebel et al., 1998; Kastner et al., 1998; Wandell, 1999; Grill-Spector et al., 2000; Tootell and Hadjikhani, 2001; Wade and Wandell, 2002; Huk et al., 2002). This has led to the paradoxical situation that, although 10 years ago virtually nothing was known about the retinotopic organization of human visual cortex, currently it has been mapped in a more systematic way than that of non-human primates. Actually, using fMRI it became possible to obtain detailed retinotopic maps and to identify areal boundaries from a considerable portion of the visual cortex of single human subjects. In the present study, we exploited these advantages of whole-brain in-vivo imaging techniques and applied them to monkeys. Because response properties might vary significantly between awake and anaesthetized animals (e.g. Pack et al., 2001), and since higher tier areas (V4, MST, IPS, TE) are more difficult to activate under anesthesia (Rainer et al., 2001), we decided to perform the experiments in awake rather than anaesthetized monkeys (Logothetis et al., 1999; Brewer et al., 2002). Moreover, the use of exactly the same imaging technique in the two primate species enables to make direct comparisons between monkey and human imaging results. Such an approach in which only the species, but not their state, is different allows to make straightforward inferences about potential analogies and homologies of visual areas.

Beside the validation of the boundaries of early areas (V1, V2, V3), we tried to isolate V3A, MT/V5 and TEO based upon their presumptive representation of the complete contralateral hemifield (Van Essen et al., 1981; Gattass and Gross, 1981, 1988; Gaska et al., 1988; Boussaoud et al., 1991). Furthermore, we focused upon the retinotopic organization of the cortex between the anterior banks of the lunate (LUS) and inferior occipital sulcus (IOS) and the posterior bank of the superior temporal sulcus (STS). This large cortical region covering and surrounding the prelunate

gyrus is classically assigned to be area 'V4' (Zeki, 1977a). However, because of the pronounced receptive field scatter, increasing receptive field sizes, and heterogeneity of response properties in this region (Zeki, 1977a; Schein et al., 1982; Maguire and Baizer, 1984; Tanaka et al., 1986; Gattass et al., 1988; Kaas and Lyon, 2001; Pigarev et al., 2002), the exact retinotopic organization of this area is still debated in monkeys. In particular the anterior border of 'classical' V4 is still controversial as it is not clear *whether* (Van Essen and Zeki, 1978; Maguire and Baizer, 1984; Brewer et al., 2002; Pigarev et al., 2002), or *not* (Gattass et al., 1988; Lyon and Kaas, 2002) this area is rostrally bordered by a representation of the horizontal meridian. Some authors (Brewer et al., 2002) added confusing to this debate by assigning either a horizontal (their Fig. 8), or a vertical meridian (their Fig. 14) as anterior border of ventral V4 within a single study. Several authors (Shipp and Zeki, 1995; Kaas and Lyon, 2001; Pigarev et al., 2002) even proposed to subdivide this relatively large extrastriate region surrounding the prelunate gyrus into distinct areas. Finally, in humans, there seems to be a distinct asymmetry between dorsal and ventral V4 (Sereno et al., 1995; Van Oostende et al., 1997; Tootell and Hadjikhani, 2001). Since preliminary evidence indicated a similar functional asymmetry between the dorsal and ventral subdivision of monkey V4 (Nelissen et al., 2000; Fize et al., 2001), we also wanted to clarify whether the latter two regions have a distinct retinotopic organization.

In the present study, we used static wedge-stimuli confined to the respective portion of the visual field. In an attempt to drive as many areas as possible, each epoch contained randomly alternating colored and achromatic checkerboards, as well as moving dots or lines. Areal boundaries were based upon the representations of the vertical and horizontal meridian, and the upper and lower visual field. Finally, a small central stimulus (1.5 degrees radius), in combination with static concentric annuli covering different eccentricities, were presented in order to define eccentricity lines in the early visual areas. This also allowed us to calculate magnification factors for striate cortex.

RESULTS

Four macaque monkeys (M1,3-5) were scanned in a horizontal bore of a 1.5T MR scanner while they were rewarded to fixate within in 2 x 2 degree window. The behavior of the monkeys was monitored on-line by recording eye positions inside the magnet. To boost the contrast-to-noise ratio of the fMRI signals (Vanduffel et al., 2001a; Leite et al., 2002), we injected intravenously a contrast agent (monocrystalline iron oxide nanoparticle, MION) prior to each scan session.

Behavior

To obtain accurate retinotopic maps in awake animals, it is essential that the subjects fixate as precisely as possible during the acquisition of the functional volumes. Therefore, we included only those time series in the statistical analysis in which the monkeys fixated more than 80% of the total scan duration within a fixation window of 2 X 2 degrees. Typically, the monkeys only used a fraction of the fixation window. However, due to minor artifacts upon the eye-movement signals that were induced by switching of the gradients during echo-planar imaging, we kept the fixation window slightly larger than needed.

Furthermore, for those runs that were incorporated in the statistical analysis, we removed saccadic eye-movement related activity by including the recorded eye-traces as a variable-of-no-interest in the general linear model (for details see Vanduffel et al., 2001a). The total number of functional volumes used for the first series of experiments was 11160 (M1), 6840 (M3), 5760 (M4), 8100 (M5). These volumes were acquired during 4, 3, 3 and 5 scanning sessions, respectively. 12000 volumes were acquired during 7 pilot sessions.

Results will be presented as t-score maps for each stimulus comparison (using SPM99). These significance maps were painted upon the reconstructed flattened hemispheres of each animal using Freesurfer. The flattened representations include the entire occipital pole of the cortex, which was cut anterior to the most rostral tips of the superior temporal sulcus and intraparietal sulcus. The operculum was split along its representation of the horizontal meridian. This cut extended medially towards the anterior end of the calcarine sulcus. To asses the variability of the maps we will present detailed data from all 8 hemispheres tested.

Representation of meridians and quadrants.

Striate and prestriate cortex

At the earliest levels of the visual cortex, the transition between areas is characterized by the representation of meridians. Therefore, to identify the borders of these early areas, we first mapped the cortical representation of the horizontal and vertical meridians. The comparison of activity evoked by the vertical and horizontal wedges revealed a stripe-like alternating pattern of higher HM-related (yellow color-coded t-map) and VM-related (blue color-coded t-map) activity (see Figs. 1 A and 2). The overlying solid (HM) and dashed (VM) white lines correspond to the areal boundaries. These boundaries were derived by combining information from the statistical maps together with local maxima in % MR signal change evoked by the horizontal or vertical wedges relative to the no-stimulus condition. These local maxima were defined by plotting the % signal change evoked by the horizontal and vertical wedges along lines running roughly perpendicular to the aforementioned alternating bands of HM and VM related activity. This is exemplified in Figs 1F and G, for monkey M1 and M3, respectively. The local maxima are indicated by the letters a-j in Figs. 1D-G. As one would expect from the electrophysiology, we could define in dorsal- and ventral occipital cortex of the 4 monkeys (see Fig. 2) the anterior borders of areas V1 (first VM representation), V2 (second HM) and V3 (second VM).

Area 'V4'

In dorsal occipital cortex, we observed in the anterior bank of the lunate sulcus and/or the prelunate gyrus three representations of a vertical meridian (see labels 1, 2 and 3 in Fig. 1A). A first long one running along a dorso-ventral axis from the anterior bank of the lunate towards the parieto-occipital sulcus (see Figs. 1A and 2). This long dorso-ventral VM within the lunate sulcus separated dorsal V3 from dorsal V4 (Zeki, 1977b) and more dorsally from V3A (see below, and Zeki, 1978; Felleman and Van Essen, 1987; Gattass et al., 1988). The two other VM representations ran roughly perpendicular to the first one, crossing the prelunate gyrus into the STS.

Although the posterior border of dorsal V4 with V3d could be identified reliably by this representation of a vertical meridian, its other borders are less clear. In most hemispheres, the portion of the prelunate gyrus belonging to V4d is predominantly driven by stimuli presented along the vertical meridian. In 6 out of 8 hemispheres, the dorsal border of V4d appears to be a representation of the vertical meridian running perpendicular to the vertical meridian between V3d and V4d (2 in Fig. 1A, see also Fig. 3 and discussion) This VM meridian has also been described by Gattass et al., 1988 (their Fig. 8). The anterior border of V4d is conventionally defined by a peripheral HM representation within the STS and abuts area V4t or V4A, (Zeki, 1971; Zeki, 1977b; Gattass et al., 1988). However, we did not find a consistent representation of a horizontal meridian in that region, except for the most central portion of V4 (representing the foveal visual field). Since we were able to map the anterior and posterior borders of V3 which is only 3-5 mm wide, it is unlikely that we cannot resolve a representation of the HM in the cortex between V4d and MT/V5.

In all hemispheres, the posterior border of V4v could be identified based upon a representation of a vertical meridian. About 7-9 mm more anteriorly, we consistently observed a HM representation between the inferior occipital sulcus (IOS) and the posterior middle temporal sulcus (PMTS) (see Figs. 1A, 2 and 4). As described by Boussaoud et al. (1991), this HM representation is fractionated. The latter representation of the horizontal meridian corresponded to the anterior border of V4v with TEO (Boussaoud et al., 1991). The dorsal extension of this anterior HM border of V4v curved away from the prelunate gyrus into the superior temporal sulcus (STS) to become the horizontal meridian between the upper and lower field representation in MT/V5 (Figs. 1C, 3B-C, and 4).

MT/V5 and FST

Area MT/V5 exhibited a robust retinotopic organization with a horizontal meridian separating a ventral upper and dorsal lower visual field representation (see Figs. 1C and 3). More

ventrally within the STS, area MT/V5 was separated from FST by a representation of a vertical meridian (see Figs. 1A, 2, 3 and 4). Dorsal from MT/V5, another vertical meridian was observed in 6 out of 8 hemispheres (Fig. 3B). In some hemispheres (e.g. M4 and M5, see Fig. 2C-D), the two representations of the vertical meridian fused to surround MT/V5 at its posterior border. Similar as observed in electrophysiological experiments (Van Essen et al., 1981; Desimone and Ungerleider, 1986; Maunsell and Van Essen, 1987; Albright and Desimone, 1987), we found quite some variability in the exact representation of these VM's surrounding MT/V5.

V3A

The most straightforward way to distinguish area V3A from its direct neighbors, is based upon its representation of the complete contralateral hemifield (Van Essen and Zeki, 1978). By presenting stimuli confined to the upper field, we could identify V3A from its direct neighbors that contain a lower visual field representation only. Indeed, anterior to the large portion of dorsal occipital cortex activated by the lower field stimulus (V1d, V2d, and V3d), an island of cortex in the anectant gyrus, that stretched towards the posterior end of the IPS, contained an upper field representation (indicated by 'U' in Figs. 1C and 2). Since V3A, represents the complete contralateral hemifield, its most caudal part comprises the small strip of cortex with a lower field representation (indicated by 'L' in Figs. 1C and 2) that lies rostral to the anterior border of V3d (VM).

In Fig. 3, this representation of the vertical meridian at the border between V3 and V3A is illustrated in detail for all hemispheres tested (see dashed white line in upper left corner of yellow inset in Figure 3A). In all cases, this VM representation was followed consecutively by a lower and upper field representation. In 50 % of the hemispheres, a horizontal meridian splitted this lower and upper field representation (at a statistical criterion of $P< 0.05$, corrected for multiple comparisons). Rostrally, V3A was bordered by a representation of the vertical meridian (in 5/8 hemispheres). Furthermore, the central visual field is represented near the ventral border of V3A (in 5/8 hemispheres). Altogether, the complete hemifield representation in this dorsal portion of the cortex could be reliably used as a fingerprint for V3A.

The upper field representation which covered the anectant gyrus within the anterior bank of the lunate sulcus, extended into the IPS (in 6/8 hemispheres). Although this is consistent with the view that V3A also covers the most caudal aspect of the IPS (Tsutsui et al., 2001), adjacent but more anterior areas within this sulcus also seem to have an upper field representation (see Figs. 1C and 3B).

Area TEO, LIP, and PO (V6)

Also area TEO, located rostral to the anterior HM border of V4v, should be distinguishable from neighboring cortex by its representation of the complete contralateral hemifield (Boussaoud et al., 1991). Contrary to V3A, however, the characteristic feature to distinguish TEO from its neighbors is a lower field representation. As marked by the arrow in Fig. 1C, we observed such a lower field representation rostral to the anterior HM border of V4v. Similarly as in the anaesthetized animal (Brewer et al., 2002), the lower field stimulus evoked relatively weak differential MR signals in this region corresponding to TEO, yet in 5 of 8 hemispheres the activation by lower field stimuli reached the statistical criterion of $P < 0.05$ (corrected for multiple comparisons). Furthermore, in agreement with the findings of Brewer et al. (2002), we observed a central visual field representation within TEO (* in Fig. 1B) in 7/8 hemispheres (see also dashed black line in Fig. 4).

Additional central visual fields representations (indicated by stars and dashed black lines, see below) were observed at the caudal-most portion of the parieto-occipital sulcus (POS) (* in Fig. 1B) and the lateral lip of the IPS. In 7 of the 8 hemispheres, an extended upper visual field representation emerged more posterior relative to this lateral foveal representation within the IPS. These localizations are in agreement with the coarse retinotopic organization of this region (Blatt et al., 1990; Ben Hamed et al., 2001), in which the foveal representation corresponds to medio-dorsal LIP, and the more peripheral representation with postero-ventral LIP (Ben Hamed et al., 2001). Only for M4 (see Fig. 3B), we observed a antero-posterior gradient from the lower to upper visual field representations as indicated by the latter authors.

Summary extrastriate cortex

Figs. 1D and E summarizes the relative positions of the meridians, and the upper and lower visual field representations with respect to the anatomical landmarks for M1 and M3. Based upon these representations, we could precisely map the borders of areas V1, V2, V3, and ventral V4. Furthermore, we were able to localize all boundaries, except for the anterior border, of areas V4d, MT/V5 and V3A. Finally, we could define at least one border of area TEO and FST.

Eccentricity mapping

Beside the polar angle maps, the second important variable of a retinotopic map is the representation of eccentricities. The combination of polar angle with eccentricity information has been used to characterize areas based upon the visual sign maps (e.g. Engel et al., 1994; Sereno et al., 1995). Furthermore, it is known that some areas are preferentially driven by peripheral presented visual stimuli (e.g. V6/PO, Galletti et al., 1999) while others have an over-representation of the fovea (e.g. TEO, Boussaoud et al., 1991). To reveal eccentricity maps throughout the visual cortex, we performed an additional experiment (in M1 and M5) in which we presented 4 sets of stimuli with the same texture patterns as used in the meridian- and quadrant mapping experiments. The first set of stimuli covered a central portion of the visual field (1.5 degrees radius). The three other sets consisted of annuli covering eccentricities from 1.5 to 3.5 degrees, from 3.5 to 7 degrees, and from 7 to 14 degrees, respectively. We acquired 4500 and 7560 functional volumes for M1 (during 1 session) and M5 (during 3 sessions), respectively. Significance maps were computed separately for each stimulus by comparing its response with the activity evoked by all remaining stimuli.

The representation of the central 1.5 degrees is illustrated by the yellow color-coded t-map in Fig. 5A. The central visual field stimulus (1.5 degrees radius) activated an ellipsoid pattern covering the most lateral portion of the operculum, and the anterior tip of the lunate and inferior occipital sulcus. Dorsally it extended along the lip of the lunate sulcus (in 5/8 hemispheres). Further rostrally, this foveal visual field representation extended from the prelunate gyrus into the STS, and ventrally it covered the prelunate gyrus up to the PMTS (see Fig. 5A). In ventral occipital cortex (V1v, V2v, V3v, and V4v), the 1.5 degree eccentricity line ran perpendicular to the areal boundaries. Dorsally, this was also the case for areas V1d, V2d and V3d. More anteriorly in dorsal V4, however, the eccentricity line turned sharply from a caudo-rostral to a more dorso-ventral course, because it links the central visual field representation of V3A with that of V4 and MT/V5. As a result, the 1.5 degree eccentricity line became parallel to the anterior border of V3 (see arrows in Fig. 5). The results for the 1.5 degree diameter stimulus are replicated for all animals (see Fig. 1B and black dashed lines in Figs. 2-4).

As the annuli covered gradually larger eccentricities (panels 5B-D), the corresponding ring of activity expanded dorsally and ventrally in the operculum, lunate sulcus, IOS and prelunate gyrus. More peripheral visual stimulation (panel D) resulted in progressively more dorso-caudal activations within the STS (probably corresponding to MSTd), as well as the anterior bank of the parieto-occipital sulcus (corresponding to areas PO/V6/V6A) and posterior parietal cortex including CIPS and 7a. This might reflect the neuronal sensitivity for large and/or eccentric stimuli in those areas. Similar to the course of the 1.5 degree eccentricity line, the lines corresponding to larger eccentricities ran perpendicular to the areal boundaries within areas V1, V2, V3 and V4v. A quite different pattern emerged in dorsal V4. Rostral to the vertical meridian border between V3d and V4d, the eccentricity lines bended sharply in a ventral direction and became nearly parallel to the areal boundaries. This resulted in a severe compression of mid- eccentricity representations within dorsal V4 (Fig. 5A-C, see also Figs. 6 and 7). Interestingly, only when stimuli larger than 7 degrees radius were used, regions in dorsal prelunate, posterior parietal and dorsal STS cortex were activated.

Using the data from the eccentricity mapping, we could calculate magnification factors for area V1. To this end, we plotted % MR signal changes for all eccentricity stimuli tested relative to a no-stimulus baseline condition. The plots were measured from ventral to dorsal locations at 3 mm intervals along two lines that ran parallel to the V1-V2 border as indicated in Fig. 6A. Then, we defined the intersections of the activity profiles from neighboring stimuli (see vertical dashed lines in Fig. 6B). The extent of cortex within V1 that was activated by each annulus was defined as the distance between two consecutive intersections. This way, we measured that the 1.5-3.5 degree stimulus activated 7 mm, and the 3.5-7 degree stimulus activated 6.5 mm of cortex. Thus for the average eccentricity of the two annuli (2.5 and 5.25 degrees, respectively) the magnification factors were respectively 3.5 and 1.9 mm/deg. These values are in close agreement with magnification factors reported by Tootell et al., (3.4 mm/deg and 2.3 mm/deg), Van Essen et al. (4.0 and 1.7 mm/deg), and the average of the other studies reported by Tootell et al. (1988) (3.6 mm/deg and 2 mm/deg at 2.5 and 5.3 degrees eccentricity respectively).

DISCUSSION

The stimuli used here were efficient to drive multiple visual areas. It has been argued that the 'phase encoded, or traveling wave' method might be less suited to detect the retinotopic organization within motion sensitive regions (Bartels and Zeki, 2000). Only recently, one could define subcomponents of the human MT/V5+ complex using this method (Huk et al., 2002). In the present study, we found in all hemispheres tested a robust retinotopic organization in MT/V5 and surrounding areas. In general, however, the maps for areas V1, V2, V3, V3A and V4v are similar to the retinotopic maps observed in humans, irrespective the 'traveling wave' or the same methodology as in the present experiment was used in the human studies. This is in agreement with a recent study, which indicated a high level of similarity between the early visual areas of humans and monkeys (Vanduffel et al., 2002).

An important technical issue when performing retinotopic experiments in awake monkeys is the accuracy of fixation. This was achieved by the extended training of the subjects: subjects M1, M3 and M4 were trained for 4-1 years prior the present experiments and participated in a number of other passive viewing experiments (e.g. Nelissen et al., 2000; Fize et al., 2001; Mandeville et al., 2001; Vanduffel et al., 2001a; Vanduffel et al., 2001b; Denys et al., 2002; Vanduffel et al., 2002). By and large, the direct measurements of eye movements, and the exclusion of saccadic related activity in the statistical analysis were effective tools to enhance the quality of the results. Finally, both signal strength and spatial specificity of the MR signals at 1.5T were significantly boosted by using a contrast agent (Vanduffel et al., 2001a; Leite et al., 2002).

Areas V1, V2 and V3

The overall retinotopic organization observed in the four monkeys was in large agreement with previously described areal boundaries and the representation of quadrants (Daniel and Whitteridge, 1961; Gattass et al., 1981; Van Essen et al., 1984).

Area V3 had a mirror-representation of area V2, as reported by Gattass et al., 1981b; Gattass et al., 1988; Felleman et al., 1997, and Lyon and Kaas, 2002. The retinotopic organization in macaque V3 is essentially equivalent to that in human V3, except for one feature. In human V3, the polar angle magnification matches that in adjacent V2. Macaque V3, however, is rather small in width reflecting its reduced polar angle magnification (Tootell et al., 1997; Lyon and Kaas, 2002). Our V3 maps were slightly wider than usually drawn (e.g. Felleman and Van Essen, 1991). An old controversy in macaque is whether 'V3d' and 'V3v/VP' are 'different' cortical areas (Burkhalter and Van Essen, 1986; Felleman and Van Essen, 1987) or two parts of one single area with an upper and ventral visual field representation (Gattass et al., 1988; Kaas and Lyon, 2001). We could not find asymmetric retinotopic properties between the two areas, adding evidence to the suggestion that V3d and V3v/VP belong to the same area (Lyon and Kaas, 2002).

Prelunate gyrus and surrounding cortex

Despite a difference in motion-sensitivity (Gaska et al., 1988; Tootell et al., 1997; Goebel et al., 1998; Sunaert et al., 1999; Vanduffel et al., 2001a), human and macaque V3A showed a remarkably similar retinotopic organization. A characteristic upper and lower visual field representation, separated by an horizontal meridian, was in agreement with earlier electrophysiological studies (Zeki, 1971; Zeki, 1977b; Van Essen and Zeki, 1978; Gattass et al., 1988). Similar to our observations, Zeki, 1978 described a representation of a vertical meridian as posterior and anterior border of this area.

A recurrent feature of the anterior bank of the lunate sulcus and prelunate gyrus was the extensive vertical meridian representation. A few electrophysiological studies have suggested a vertical meridian representation on the prelunate gyrus (Maguire and Baizer, 1984; Youakim et al., 2001). Furthermore, the pattern of degeneration after callosal section covers this part of the prelunate gyrus (Zeki 1977a, Desimone et al., 1993). It is known that the corpus callosum interconnects primarily regions representing the vertical meridian (Van Essen and Zeki, 1978). Also anterograde tracers injected along the VM representation in V1 (Lyon and Kaas, 2002), as well as retrograde tracers injected along the vertical meridian representation in area MT/V5 (Ungerleider and Desimone, 1986) labeled this portion of the prelunate gyrus (see also Van Essen et al., 1982). Thus, based upon this electrophysiological and connectional patterns, one would expect a vertical meridian representation exactly where we observed one using our fMRI methods. On should note that given the RF size and scatter, the VM and HM stimuli will also drive a number of neurons with RFs along the diagonal, as confirmed by a direct test with such diagonal wedges (data not shown).

The region dorso-medial to the VM representation perpendicular to the rostral border of V3 (number 2 in Fig. 1A) receives input from the anterior bank of the parieto-occipital sulcus (Colby et al., 1988), while inferotemporal cortex is more heavily connected with the region ventro-lateral to this VM (Morel and Bullier, 1990; Boussaoud et al., 1991). Furthermore, the dorso-medial but not the ventro-lateral region projects to area 7a (Andersen et al., 1990). Thus, it is tempting to ask the question whether this portion of the prelunate gyrus can be subdivided into a dorso-medial and ventro-lateral area divided by a representation of a VM. Differential functional properties at both sides of this VM would further support this idea. In a recent fMRI study, we found sensitivity for the 3D-structure-from-motion ventrally but not dorsally relative to this VM on the prelunate gyrus (Vanduffel et al., 2002). Furthermore, several electrophysiological studies found a high proportion of orientation-sensitive cells dorso-*medial* to the vertical meridian representation, and a much lower proportion ventro-lateral to it (Van Essen and Zeki, 1978; Schein et al., 1982; Mountcastle et al., 1987; Youakim et al., 2001). Thus, retinotopically, functionally, as well as anatomically, there is substantial evidence to assign this VM (2 in fig 1A) as dorsal border of V4. The next question is to what region the dorso-medial prelunate area might correspond to? In the present study, we could barely drive this region. The only exception was when we used large peripheral stimuli (Fig. 5D). The latter finding is in agreement with the electrophysiological finding of Tanaka and colleagues (Tanaka et al., 1986), which could drive the dorso-medial aspect of the prelunate sulcus (their area 'PVA'), mainly with large peripheral stimuli. As suggested by Gattass et al., 1988 and Andersen et al., 1990 this dorsal portion of the prelunate gyrus might correspond to area DP.

Ventro-lateral to this border with presumed DP, the organization of the prelunate gyrus is also questionable. Based upon connection patterns and retinotopy, this region of cortex was originally called V4. Subsequently, several subdivision schemes have been proposed along the caudo-rostral axis. For example, based upon a representation of a horizontal meridian, V4 was further subdivided into V4 proper and V4A (Zeki, 1971; Pigarev et al., 2002). Furthermore, Kaas and colleagues have argued that this dorsal portion of V4 corresponds to DL of New World monkeys, and subdivided this area in a rostral (DLr) and a caudal (DLc) part (Kaas, 1996). At least with the present resolution of our technique, we obtained no evidence for a caudo-rostral subdivision of dorsal V4. We did find a horizontal meridian as anterior border of *ventral* V4 which extended dorsally towards the horizontal meridian splitting the lower and upper visual field of MT/V5. Thus only for V4v, and at best the most central portion of V4 (V4c), we found evidence for a horizontal meridian forming the anterior border of V4. In agreement with the electrophysiological maps of Gattass et al., 1988 and the connection patterns of Lyon and Kaas,

2002, we could not observe a horizontal nor a vertical meridian as anterior border for the most dorsal portion of V4 (though still ventral relative to the V4/DP-border as described above). It is noteworthy that electrophysiological studies revealed a large variability in the representation of the meridians at this level, and even when present, they corresponded to very few neurons (Van Essen et al., 1981; Desimone and Ungerleider, 1986; Maunsell and Van Essen, 1987; Gattass et al., 1988).

Area V4 showed another striking difference between the representation of the upper and lower visual fields in its ventral and dorsal part, respectively. While the iso-eccentricity lines ran perpendicular to the representations of the meridians within V4v, this was not true for V4d. From an almost perfect caudo-rostral axis in areas V1d, V2d and V3d, the iso-eccentricity lines curved ventrally within V4d, running almost parallel to its posterior border. This pattern of iso-eccentricity lines is highly comparable with that found in electrophysiological mapping experiments (Gattass et al., 1988, see Fig. 7A), and our earlier fMRI study (Fig 1A of Vanduffel et al., 2002). It also indicates that the assumption made for the 'traveling wave' method that the angular and eccentricity representations must run in locally orthogonal directions in order to segment cortical regions into different areas (Brewer et al 2002, Wade et al 2002), is unsafe. This assumption is clearly not met in V4d. It is even questionable whether this is also the case for areas containing a full contralateral hemifield representation such as V3A, TEO and MT/V5.

These differences in retinotopic organization between ventral and dorsal V4 might indicate that other functional differences between these areas exist.

MT/V5 and FST

In the present study, we first localized area MT/V5 based upon its motion sensitivity (Vanduffel et al., 2001a). The retinotopic organization within this area matched closely the organization as found in previous electrophysiological studies (Van Essen et al., 1981; Desimone and Ungerleider, 1986; Maunsell and Van Essen, 1987). The representation of a horizontal meridian separated a dorsal lower field from a ventral upper visual field representation. Similarly as V3A which also contains a representation of the complete contralateral hemifield, MT/V5 is dorsally and ventrally bordered by a vertical meridian representation. Furthermore, the representation of the foveal visual field within MT/V5 is located below the peripheral field, in line with the observations of Maunsell and Van Essen, 1987. As described by Desimone and Ungerleider, 1986, and Gattass et al., 1988 (see Figure 7), both the eccentricity lines and polar angle representations continue between V4 and MT/V5. The retinotopic organization in this portion of the STS, is also in complete agreement with results from the recent anterograde tracer study by Lyon and Kaas, 2002. Injection of tracer along the representation of the horizontal meridian within area V1 resulted in anterograde labeling in the middle of MT/V5. Injecting tracer in striate cortex at the representation of the lower vertical meridian labeled the dorsal portion of MT/V5, while a V1 injection near the upper vertical meridian resulted in anterogradely transported label in ventral MT/V5 (immediately ventral relative the HM representation). Also Maunsell and Van Essen, 1987 observed significant callosal input to this portion of MT/V5.

TEO

The mild tendency for a lower field dorsally and upper field ventrally in TEO fits with the electrophysiological findings of Boussaoud et al. (1991). Although neurons of TEO are known to be driven by upper or lower field stimuli, our inability to reveal a robust retinotopic organization indicates that neurons with receptive fields driven by upper or lower field stimuli might be heterogeneously distributed (see also Boussaoud et al., 1991), or that our stimuli were not suitable enough to drive this region (Hikosaka, 1998).

Conclusion

Using low-field fMRI in awake monkeys, we can identify a significant part of the visual cortex which is a prerequisite to interpret data from future fMRI experiments within the same subjects. Reliable retinotopic signals were obtained from areas as small as V3 (only 3-5 mm wide). The significant retinotopic differences between dorsal and ventral V4 might imply a different functional role for these areas. Future fMRI and electrophysiological follow-up studies in the

monkey might resolve whether the functional properties between dorsal and ventral V4 are dissimilar enough to consider them distinct areas.

EXPERIMENTAL PROCEDURES

Four male (M1, M3, M4 and M5) rhesus monkeys (4-6 kg) were used in the first experiment and two (M1 and M5) in the second experiment. The surgical procedures and training of the animals was similar to Vanduffel et al., 2001a and are briefly described here. Prior to MR scanning, each monkey was implanted with a MR-compatible plastic headset, which was covered by dental acrylic. All operations were performed under isoflurane (1.5%) / N_2O (50%) / O_2 (50%) anesthesia. Antibiotics (50 mg/kg i.m., Kefzol®, Lilly, Brussels) and analgesics (4 mg/kg i.m. Dolzam®, Zambon, Brussels) were given daily for 3-7 days following each surgery. The surgical procedures conformed to national, European and NIH Guidelines for the care and use of laboratory animals.

After recovery, the monkeys were adapted to restraint in a plastic chair, then habituated to the sounds of MR scanning in a 'mock' MR bore. The monkeys were seated comfortably on their haunches, in the so-called 'sphinx' position. The monkeys were water-deprived during the period of testing, and behavioral control was achieved using operant conditioning techniques. They were trained to a high acuity orientation discrimination task used to accurately calibrate a pupil/corneal reflection tracking system (RK-726PCI, Iscan Inc, Cambridge, MA). Once this eye-tracking system was calibrated, we presented a fixation spot only. The monkey was rewarded for maintaining fixation within a square-shaped central fixation window (2° on a side). The interval between rewards was systematically decreased (from 2500 to 500 ms) as the monkey maintained his fixation within the window. After fixation performance reached asymptote (after 20-50 training sessions), each monkey in its plastic restraint box was placed into a horizontal bore, 1.5 T Siemens Sonata scanner, equipped with echo-planar imaging. A radial surface coil (10 cm diameter) was positioned immediately over the head. This coil covered sufficiently the whole monkey brain. Before the scanning, MION (4-11 mg/kg), diluted in an isotonic sodium citrate (pH 8.0), was injected intravenously into the femoral vein.

Visual stimuli were projected from a Barco 6300 LCD projector (1024 x 768 pixels, 60 Hz refresh rate) using customized optics (Buhl Optical), onto a screen which was positioned 54 cm in front of the monkey's eyes. In the first experiment, five types of stimuli were used: (1) a 12° wedge, centered on the horizontal meridian axis and symmetric with respect to the fixation point (referred to as “horizontal meridian” stimulus); (2) a 24° wedge, centered on the vertical meridian axis and symmetric with respect to the fixation point (“vertical meridian” stimulus); (3) a 168° wedge, symmetric with respect to the upper vertical meridian axis (“upper visual field” stimulus); (4) a 168° wedge, symmetric to the lower vertical meridian axis (“lower visual field” stimulus); and (5) a central disk (3° diameter) referred to as “central visual field” stimulus. In the second experiment, the “central visual field” stimulus was used in addition to three annuli centered on the fixation point, with respective inner and outer radii of [1.5-3.5], [3.5-7], [7-14]° degrees eccentricity. All these stimuli were composed of four different textures randomly alternating each 0.9s : a colored flickering checkerboard (flickering at 4 Hz), an achromatic flickering checkerboard (same refresh rate), moving white dots (0.25° diameter, speed 4° per second, 10% dot density), and moving white lines (0.1° thickness, same speed and density).

A block design was used in each scan session (block durations 24 seconds). Only scan sessions where the behavioral performance of the monkeys was excellent (> 80% fixation of the total scan duration) were considered for statistical analysis. Each functional scan (time series) consisted of gradient-echo echoplanar whole-brain images (EPI; TR 2.4s; TE = 28 ms; 64 x 64 matrix; 2 x 2 x 2 mm voxels; 32 sagittal slices) using a Siemens Vision MR 1.5 Tesla scanner. In a separate session, an anatomical 3D-MPRAGE volume (1 x 1 x 1 mm voxel size) was acquired using a knee-coil while the monkey was anaesthetized. These anatomical volumes were placed in the Horsley-Clark stereotaxic space.

The functional volumes were aligned to correct for brain motion, then non-rigidly co-registered with their own anatomical volumes using the ‘MATCH’ software. Briefly, the algorithm computed a dense deformation field by composition of small displacements minimizing a local

correlation criterion. The use of a local similarity measure allowed to cope with non-stationary behaviors in the intensity profiles of the anatomical and functional volumes. Regularization of the deformation field was achieved by low-pass filtering. Details regarding this approach can be found in Chefd'hotel et al., 2002 and Hermosillo et al., 2002. The functional volumes were further resliced to 1 mm^3 voxels and smoothed with an isotropic Gaussian kernel (sigma 0.68 mm).

Data were analyzed using standard SPM99 procedures (global scaling, low and high-pass filtering). Each stimulus epoch was represented as a box-car model convoluted by the MION response function defined in Vanduffel et al. 2001. The remainder of the analysis was similar to this previous study. The t-score maps were thresholded at $P<0.05$ corrected for multiple comparisons, corresponding to a t-score > 4.86. For the coronal sections of the Figs. 3 and 4, the thresholds were increased to visualize optimally the localization of the most significant voxels ($t>10$, 20 or 40, thresholds are indicated on the color-scalebars). The sign of the percent MR signal change (Figs. 1F, G and 6) is inverted for convenience (an increase in blood volume as measured by MION leads to a decrease in MR signal). T-score maps were combined and projected to the flattened cortical reconstruction of the same animal using Freesurfer software.

REFERENCES

Albright, T.D., and Desimone, R. (1987). Local precision of visuotopic organization in the middle temporal area (MT) of the macaque. Exp.Brain Res. 65:582-592.

Andersen, R.A., Asanuma, C., Essick, G., and Siegel, R.M. (1990). Corticocortical connections of anatomically and physiologically defined subdivisions within the inferior parietal lobule. J.Comp.Neurol. 296:65-113.

Bartels, A., and Zeki, S. (2000). The architecture of the colour centre in the human visual brain: new results and a review. Eur.J.Neurosci. 12:172-193.

Ben Hamed, S., Duhamel, J.R., Bremmer, F., and Graf, W. (2001). Representation of the visual field in the lateral intraparietal area of macaque monkeys: a quantitative receptive field analysis. Exp.Brain Res. 140:127-144.

Blatt, G.J., Andersen, R.A., and Stoner, G.R. (1990). Visual receptive field organization and cortico-cortical connections of the lateral intraparietal area (area LIP) in the macaque. J.Comp.Neurol. 299:421-445.

Boussaoud, D., Desimone, R., and Ungerleider, L.G. (1991). Visual topography of area TEO in the macaque. J.Comp.Neurol. 306:554-575.

Boussaoud, D., Ungerleider, L.G., and Desimone, R. (1990). Pathways for motion analysis: cortical connections of the medial superior temporal and fundus of the superior temporal visual areas in the macaque. J.Comp.Neurol. 296:462-495.

Brewer, A.A., Press, W.A., Logothetis, N.K., and Wandell, B.A. (2002). Visual areas in macaque cortex measured using functional magnetic resonance imaging. J.Neurosci. 22:10416-10426.

Burkhalter, A., and Van Essen, D.C. (1986). Processing of color, form and disparity information in visual areas VP and V2 of ventral extrastriate cortex in the macaque monkey. J.Neurosci. 6:2327-2351.

Chefd'hotel, C., Hermosillo, G., and Faugeras, O. Flows of diffeomorphisms for multimodal image registration. Proceedings of IEEE International Symposium on Biomedical Imaging . 7-8-2002.

Colby, C.L., Gattass, R., Olson, C.R., and Gross, C.G. (1988). Topographical organization of cortical afferents to extrastriate visual area PO in the macaque: a dual tracer study. J.Comp.Neurol. 269:392-413.

Daniel, P.M., and Whitteridge, D. (1961). the representation of the visual field on the cerebral cortex in monkeys. J.Physiol. 203-221.

Denys, K., Vanduffel, W., Fize, D., Peuskens, H., Nelissen, K., Vandenbergue, R., and Orban, G.A. (2002). The lateral occipital complex in the monkey and the human. Soc.Neurosci.Abstr. 2002:161.1

Desimone, R., Moran, J., Schein, S.J., and Mishkin, M. (1993). A role for the corpus callosum in visual area V4 of the macaque. Vis.Neurosci. 10:159-171.

Desimone, R., and Ungerleider, L.G. (1986). Multiple visual areas in the caudal superior temporal sulcus of the macaque. J.Comp.Neurol. 248:164-189.

DeYoe, E.A., Carman, G.J., Bandettini, P., Glickman, S., Wieser, J., Cox, R., Miller, D., and Neitz, J. (1996). Mapping striate and extrastriate visual areas in human cerebral cortex. Proc.Natl.Acad.Sci.U.S.A. 93:2382-2386.

Engel, S., Glover, G.H., and Wandell, B. (1997). Retinotopic organization in human visual cortex and the spatial precision of functional MRI. Cerebr. Cortex 7: 181-192.

Engel, S.A., Rumelhart, D.E., Wandell, B.A., Lee, A.T., Glover, G.H., Chichilnisky, E.J., and Shadlen, M.N. (1994). fMRI of human visual cortex. Nature 369:525

Felleman, D.J., Burkhalter, A., and Van Essen, D.C. (1997). Cortical connections of areas V3 and VP of macaque monkey extrastriate visual cortex. J.Comp.Neurol. 379:21-47.

Felleman, D.J., and Van Essen, D.C. (1987). Receptive field properties of neurons in area V3 of macaque monkey extrastriate cortex. J.Neurophysiol. 57:889-920.

Felleman, D.J., and Van Essen, D.C. (1991). Distributed hierarchical processing in the primate cerebral cortex. Cereb.Cortex. 1:1-47.

Fize, D., Vanduffel, W., Nelissen, K., Van Hecke, P., Mandeville, J.B., Tootell, R.B., and Orban, G.A. (2001). Distributed processing of kinetic boundaries in monkeys investigated using fMRI. Soc.Neurosci.Abstr. 27: 11.10

Galletti, C., Fattori, P., Gamberini, M., and Kutz, D.F. (1999). The cortical visual area V6: brain location and visual topography. Eur.J.Neurosci. 11:3922-3936.

Gaska, J.P., Jacobson, L.D., and Pollen, D.A. (1988). Spatial and temporal frequency selectivity of neurons in visual cortical area V3A of the macaque monkey. Vision Res. 28:1179-1191.

Gattass, R., and Gross, C.G. (1981). Visual topography of striate projection zone (MT) in posterior superior temporal sulcus of the macaque. J.Neurophysiol. 46:621-638.

Gattass, R., Gross, C.G., and Sandell, J.H. (1981). Visual topography of V2 in the macaque. J.Comp.Neurol. 201:519-539.

Gattass, R., Sousa, A.P., and Gross, C.G. (1988). Visuotopic organization and extent of V3 and V4 of the macaque. J.Neurosci. 8:1831-1845.

Goebel, R., Khorram-Sefat, D., Muckli, L., Hacker, H., and Singer, W. (1998). The constructive nature of vision: direct evidence from functional magnetic resonance imaging studies of apparent motion and motion imagery. Eur.J.Neurosci. 10:1563-1573.

Grill-Spector, K., Kushnir, T., Hendler, T., and Malach, R. (2000). The dynamics of object-selective activation correlate with recognition performance in humans. Nat.Neurosci. 3:837-843.

Hadjikhani, N., Liu, A.K., Dale, A.M., Cavanagh, P., and Tootell, R.B. (1998). Retinotopy and color sensitivity in human visual cortical area V8. Nat.Neurosci. 1:235-241.

Hermosillo, G., Chefd'hotel, C., and Faugeras, O. (2002). Variational methods for multimodal image matching. International Journal of Computer Vision 50:329-343.

Hikosaka, K. (1998). Representation of foveal visual fields in the ventral bank of the superior temporal sulcus in the posterior inferotemporal cortex of the macaque monkey. Behav.Brain Res. 96:101-113.

Huk, A.C., Dougherty, R.F., and Heeger, D.J. (2002). Retinotopy and functional subdivision of human areas MT and MST. J.Neurosci. 22:7195-7205.

Kaas, J.H. (1996). Theories of visual cortex organization in primates: areas of the third level. Prog.Brain Res. 112:213-221.

Kaas, J.H., and Lyon, D.C. (2001). Visual cortex organization in primates: theories of V3 and adjoining visual areas. Prog.Brain Res. 134:285-295.

Kastner, S., De Weerd, P., Desimone, R., and Ungerleider, L.G. (1998). Mechanisms of directed attention in the human extrastriate cortex as revealed by functional MRI. Science 282:108-111.

Leite, F.P., Tsao, D., Vanduffel, W., Fize, D., Sasaki, Y., Wald, L.L., Dale, A.M., Kwong, K.K., Orban, G.A., Rosen, B.R., Tootell, R.B., and Mandeville, J.B. (2002). Repeated fMRI using iron oxide contrast agent in awake, behaving macaques at 3 Tesla. Neuroimage 16:283-294.

Lewis, J.W., and Van Essen, D.C. (2000). Mapping of architectonic subdivisions in the macaque monkey, with emphasis on parieto-occipital cortex. J.Comp.Neurol. 428:79-111.

Logothetis, N.K., Guggenberger, H., Peled, S., and Pauls, J. (1999). Functional imaging of the monkey brain. Nat.Neurosci. 2:555-562.

Lyon, D.C., and Kaas, J.H. (2002). Evidence for a modified V3 with dorsal and ventral halves in macaque monkeys. Neuron 33:453-461.

Maguire, W.M., and Baizer, J.S. (1984). Visuotopic organization of the prelunate gyrus in rhesus monkey. J.Neurosci. 4:1690-1704.

Mandeville, J.B., Vanduffel, W., Fize, D., Nelissen, K., Rosen, B.R., Tootell, R.B., Van Hecke, P., and.Orban, G.A. (2001). Enhanced fMRI using iron oxide contrast agent in awake, behaving primates. Proc.Intl.Soc.Mag.Reson.Med. 9:1334

Maunsell, J.H., and Van Essen, D.C. (1987). Topographic organization of the middle temporal visual area in the macaque monkey: representational biases and the relationship to callosal connections and myeloarchitectonic boundaries. J.Comp.Neurol. 266:535-555.

Morel, A., and Bullier, J. (1990). Anatomical segregation of two cortical visual pathways in the macaque monkey. Vis.Neurosci. 4:555-578.

Mountcastle, V.B., Motter, B.C., Steinmetz, M.A., and Sestokas, A.K. (1987). Common and differential effects of attentive fixation on the excitability of parietal and prestriate (V4) cortical visual neurons in the macaque monkey. J.Neurosci. 7:2239-2255.

Nelissen, K., Vanduffel, W., Sunaert, S., Janssen, P., Tootell, R.B., and.Orban, G.A. (2000). Processing of kinetic boundaries investigated using fMRI and the double-label deoxyglucose technique in awake monkeys. Soc.Neurosci.Abstr. 26:1584.

Orban, G.A., Kennedy, H., and Maes, H. (1980). Functional changes across the 17-18 border in the cat. Exp.Brain Res. 39:177-186.

Pack, C.C., Berezovskii, V.K., and Born, R.T. (2001). Dynamic properties of neurons in cortical area MT in alert and anaesthetized macaque monkeys. Nature 414:905-908.

Pandya, D.N., and Seltzer, B. (1982). Intrinsic connections and architectonics of posterior parietal cortex in the rhesus monkey. J.Comp.Neurol. 204:196-210.

Pigarev, I.N., Nothdurft, H.C., and Kastner, S. (2002). Neurons with radial receptive fields in monkey area V4A: evidence of a subdivision of prelunate gyrus based on neuronal response properties. Exp.Brain Res. 145:199-206.

Preuss, T.M., and Goldman-Rakic, P.S. (1991). Architectonics of the parietal and temporal association cortex in the strepsirhine primate Galago compared to the anthropoid primate Macaca. J.Comp.Neurol. 310:475-506.

Rainer, G., Augath, M., Trinath, T., and Logothetis, N.K. (2001). Nonmonotonic noise tuning of BOLD fMRI signal to natural images in the visual cortex of the anaesthetized monkey. Curr.Biol. 11:846-854.

Schein, S.J., Marrocco, R.T., and de Monasterio, F.M. (1982). Is there a high concentration of color-selective cells in area V4 of monkey visual cortex? J.Neurophysiol. 47:193-213.

Seltzer, B., and Pandya, D.N. (1978). Afferent cortical connections and architectonics of the superior temporal sulcus and surrounding cortex in the rhesus monkey. Brain Res. 149:1-24.

Sereno, M.I., Dale, A.M., Reppas, J.B., Kwong, K.K., Belliveau, J.W., Brady, T.J., Rosen, B.R., and Tootell, R.B. (1995). Borders of multiple visual areas in humans revealed by functional magnetic resonance imaging. Science 268:889-893.

Shipp, S., and Zeki, S. (1995). Segregation and convergence of specialised pathways in macaque monkey visual cortex. J.Anat. 187:547-562.

Stepniewska, I., and Kaas, J.H. (1996). Topographic patterns of V2 cortical connections in macaque monkeys. J.Comp.Neurol. 371:129-152.

Sunaert, S., Van Hecke, P., Marchal, G., and Orban, G.A. (1999). Motion-responsive regions of the human brain. Exp.Brain Res. 127:355-370.

Tanaka, M., Weber, H., and Creutzfeldt, O.D. (1986). Visual properties and spatial distribution of neurones in the visual association area on the prelunate gyrus of the awake monkey. Exp.Brain Res. 65:11-37.

Tootell, R.B., and Hadjikhani, N. (2001). Where is 'dorsal V4' in human visual cortex? Retinotopic, topographic and functional evidence. Cereb.Cortex 11:298-311.

Tootell, R.B., Mendola, J.D., Hadjikhani, N.K., Ledden, P.J., Liu, A.K., Reppas, J.B., Sereno, M.I., and Dale, A.M. (1997). Functional analysis of V3A and related areas in human visual cortex. J.Neurosci. 17:7060-7078.

Tootell, R.B., Switkes, E., Silverman, M.S., and Hamilton, S.L. (1988). Functional anatomy of macaque striate cortex. II. Retinotopic organization. J.Neurosci. 8:1531-1568.

Tsutsui, K., Jiang, M., Yara, K., Sakata, H., and Taira, M. (2001). Integration of perspective and disparity cues in surface-orientation-selective neurons of area CIP. J.Neurophysiol. 86:2856-2867.

Ungerleider, L.G., and Desimone, R. (1986). Cortical connections of visual area MT in the macaque. J.Comp.Neurol. 248:190-222.

Van Essen, D. C. (2002). Organization of visual areas in Macaque and human cerebral cortex. In: The Visual Neurosciences (Chalupa L, Werner JS eds), MIT Press.

Van Essen, D.C., Lewis, J.W., Drury, H.A., Hadjikhani, N., Tootell, R.B., Bakircioglu, M., and Miller, M.I. (2001). Mapping visual cortex in monkeys and humans using surface-based atlases. Vision Res. 41:1359-1378.

Van Essen, D.C., Maunsell, J.H., and Bixby, J.L. (1981). The middle temporal visual area in the macaque: myeloarchitecture, connections, functional properties and topographic organization. J.Comp.Neurol. 199:293-326.

Van Essen, D.C., Newsome, W.T., and Bixby, J.L. (1982). The pattern of interhemispheric connections and its relationship to extrastriate visual areas in the macaque monkey. J.Neurosci. 2:265-283.

Van Essen, D.C., Newsome, W.T., and Maunsell, J.H. (1984). The visual field representation in striate cortex of the macaque monkey: asymmetries, anisotropies, and individual variability. Vision Res. 24:429-448.

Van Essen, D.C., and Zeki, S.M. (1978). The topographic organization of rhesus monkey prestriate cortex. J.Physiol. 277:193-226.

Van Oostende, S., Sunaert, S., Van Hecke, P., Marchal, G., and Orban, G.A. (1997). The kinetic occipital (KO) region in man: an fMRI study. Cereb.Cortex 7:690-701.

Vanduffel, W., Fize, D., Mandeville, J.B., Nelissen, K., Van Hecke, P., Rosen, B.R., Tootell, R.B., and Orban, G.A. (2001a). Visual motion processing investigated using contrast agent-enhanced fMRI in awake behaving monkeys. Neuron 32:565-577.

Vanduffel, W., Fize, D., Nelissen, K., Van Hecke, P., Mandeville, J.B., Tootell, R.B., and.Orban, G.A. (2001b). Cue-invariant shape processing in the awake fixating monkey: a contrast-agent enhanced fMRI study. Soc.Neurosci.Abstr. 27:1110

Vanduffel, W., Fize, D., Peuskens, H., Denys, K., Sunaert, S., Todd, J.T., and Orban, G.A. (2002). Extracting 3D from motion: differences in human and monkey intraparietal cortex. Science 298:413-415.

Wade, A.R., Brewer, A.A., Rieger, J.W. and Wandell, B.A. (2002). Functional measurements of human ventral occipital cortex: retinotopy and colour. Phil. Trans. R. Soc. Lond. B 357: 963-973.

Wandell, B.A. (1999). Computational neuroimaging of human visual cortex. Ann. Rev. Neurosci. 22:145

Youakim, M., Bender, D.B., and Baizer, J.S. (2001). Vertical meridian representation on the prelunate gyrus in area V4 of macaque. Brain Res.Bull. 56:93-100.

Zeki, S.M. (1971). Cortical projections from two prestriate areas in the monkey. Brain Res. 34:19-35.

Zeki, S.M. (1977a). Colour coding in the superior temporal sulcus of rhesus monkey visual cortex. Proc.R.Soc.Lond.B.Biol.Sci. 197:195-223.

Zeki, S.M. (1977b). Simultaneous anatomical demonstration of the representation of the vertical and horizontal meridians in areas V2 and V3 of rhesus monkey visual cortex. Proc.R.Soc.Lond.B.Biol.Sci. 195:517-523.

Zeki, S.M. (1978). The third visual complex of rhesus monkey prestriate cortex. J.Physiol. 277:245-272.

FIGURES

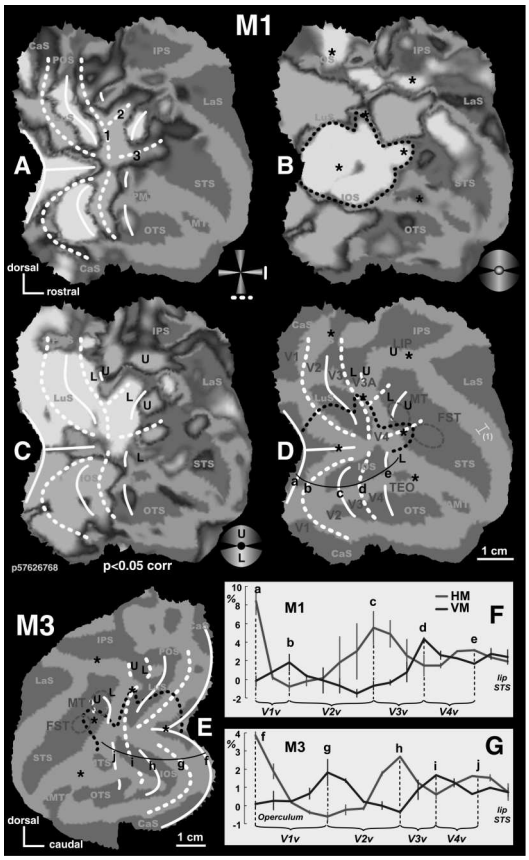

Figure 1. Representation of meridians, central and peripheral, and upper and lower visual field.

A T-score map of horizontal (red-yellow color-code) and vertical (blue color-code) meridian representations. The meridian driven activations are represented as t-score maps ($p<0.05$, corrected for multiple comparisons) on the flattened cortical reconstruction (dark grey : sulci, light grey : gyri) *White solid and dashed lines* represent the horizontal and vertical meridians, respectively. **B** Significance map for central (red-yellow) and peripheral visual stimulation (blue). *Black dashed line* indicates the contour of the central 1.5 degree eccentricity line. S*tars* indicate additional foveal activations ($p<0.05$, corrected for multiple comparisons). **C** Significance map for upper (blue) and lower (red-yellow) visual field representations. *'L' and 'U' labels* indicate the locations of lower and upper field representations. **D-E** Summary of visual field maps for M1 (right hemisphere) and M3 (left hemisphere) based upon tests as illustrated in panels A-C. Red labels indicate the visual areas defined by either anatomical location or known visual field representation (V1-4, V3A, LIP), anatomical location and motion sensitivity (MT/V5, FST). **F, G** Plots of % MR signal change related to horizontal (red) and vertical (blue) meridian relative to the no-stimulus condition as sampled along the lines indicated in panel D (a-e) and panel E (f-j). Error bars represent the standard error of the mean between the left and right hemispheres. IOS: inferior occipital sulcus, OTS: occipito temporal sulcus, STS: superior temporal sulcus, LaS: lateral sulcus, IPS: intraparietal sulcus, POS: parieto-occipital sulcus, LuS: lunate sulcus. **(1)** The extent of light grey on the anatomical representations could give a misleading estimation of the width of the gyri. A more realistic extent of the gyrus is represented by the yellow ruler in D. This remark holds true for all gyri of all flat maps.

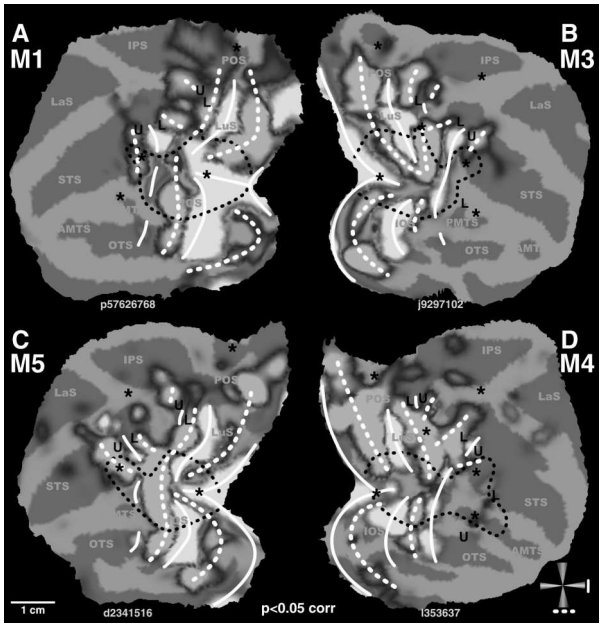

Figure 2. Representation of meridians.

T-score maps ($p<0.05$, corrected for multiple comparisons) of horizontal (red-yellow) and vertical (blue) meridian representations are presented upon the flattened cortical reconstructions of the left hemispheres of M1 and M5 and right hemispheres of M3 and M4. Same conventions as in Fig. 1.

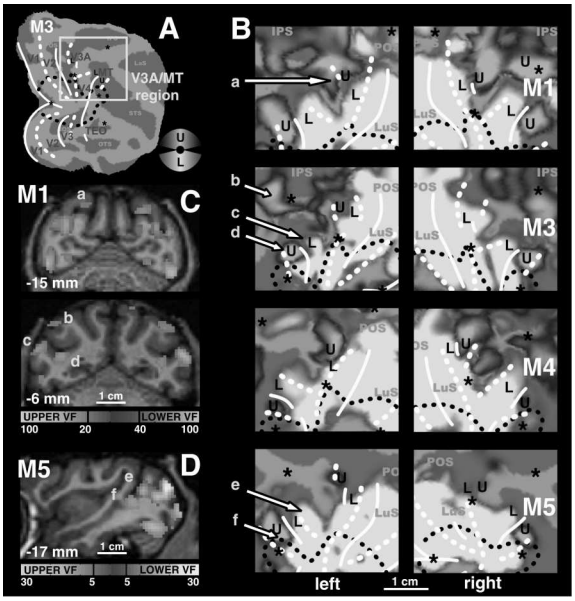

Figure 3. Lower and upper visual field representations in the dorsal anterior visual cortex.

A Summary view of the right hemisphere of M3. Same conventions as in Figs. 1 and 2. The yellow box indicates the position of the detailed activity maps of the 4 monkeys as shown in panel B. **B** Upper (blue color-code) and lower (yellow color-code) visual field representations ($p<0.05$, corrected for multiple comparisons) in the dorsal anterior cortex of the 8 hemispheres (left hemispheres is on the left, right hemisphere on the right). Yellow labels and arrows indicate locations shown in the brain sections in panels C and D. **C** Upper (blue) and lower (yellow) visual fields representations overlaid upon coronal brain sections of M1. The activities are highly thresholded to obtain good spatial specificity and to visualize the underlying anatomy. Horsley-Clarke coordinates are indicated on the left bottom of each section. Left hemisphere is on the left. Scale bars represent *t*-scores. **D** Sagittal brain section of the left hemisphere of M3 ; same conventions than C.

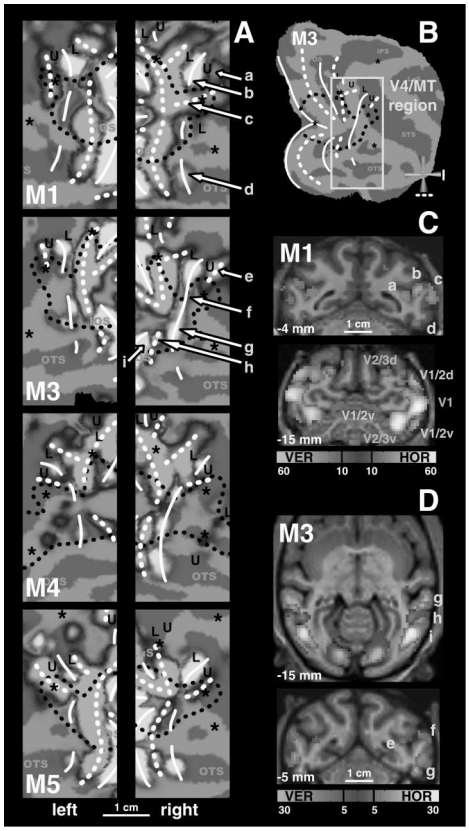

Figure 4. Horizontal and vertical meridian representations in area V4 and neighboring cortex.

A T-score maps ($p<0.05$, corrected for multiple comparisons) for horizontal (yellow code) and vertical (blue code) meridian representations are presented upon details of the flattened cortical reconstructions of the left hemispheres and right hemispheres of the 4 subjects. Same conventions as in Fig. 1. The location of the region of interest is shown in B. Yellow labels and arrows indicate locations shown in the coronal and horizontal brain sections in panels C and D. **C** Coronal brain sections of M1 showing horizontal meridian (yellow code) and vertical meridian (blue code) driven activity. The coronal section at -15 mm can be compared with the one of Fig. 3C in the same animal. **D** Horizontal and coronal brain sections of M3 ; same conventions as above.

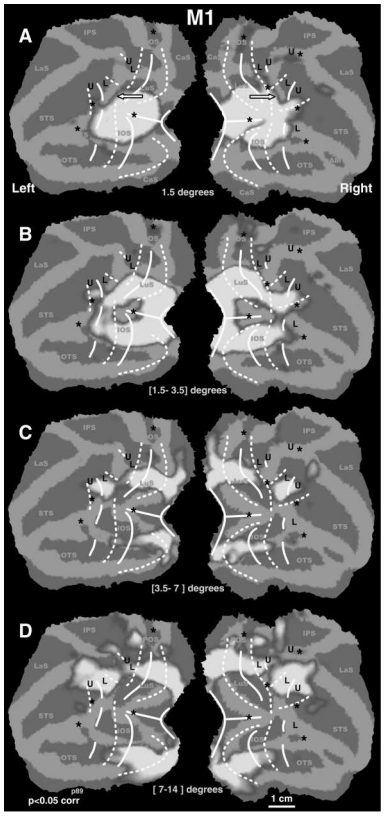

Figure 5. Eccentricity maps for left and right hemispheres of M1.

A T-score maps ($p<0.05$, corrected for multiple comparisons) for the central visual field stimulus (1.5 degree radius). **B**-**D** The activity maps revealed by annuli with a radius of [1.5-3.5], [3.5-7] and [7-14] degrees, respectively. The iso-eccentricity lines, defined by the borders of each activity pattern, were perpendicular to the meridians in the early areas. In dorsal V4, the iso-eccentricity lines run nearly parallel to the areal boundaries (see arrows). Same conventions as in Fig. 1.

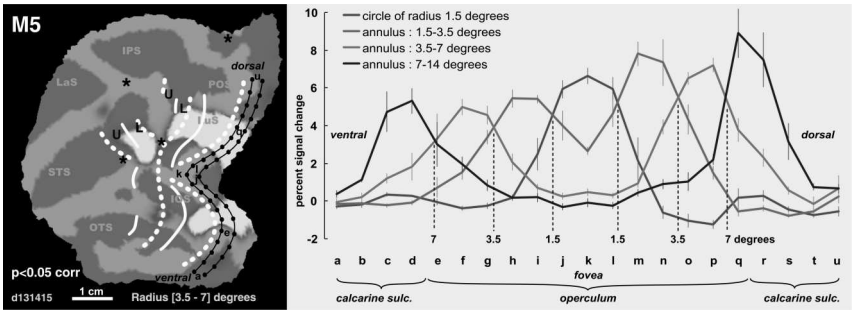

Figure 6. Eccentricity in area V1

A Significance map of the activity driven by the [3.5-7] degrees annulus in M5. The iso-eccentricity lines were very similar to those of M1. Black dots represent the sampling points (3 mm +/-0.3) along two lines running parallel to the meridians of area V1. The % signal change relative to the no-stimulus condition for the 4 different stimuli at these points are plotted in **B**. The location of 1.5, 3.5 and 7 degrees edges were defined as the intersections of the activity profiles.

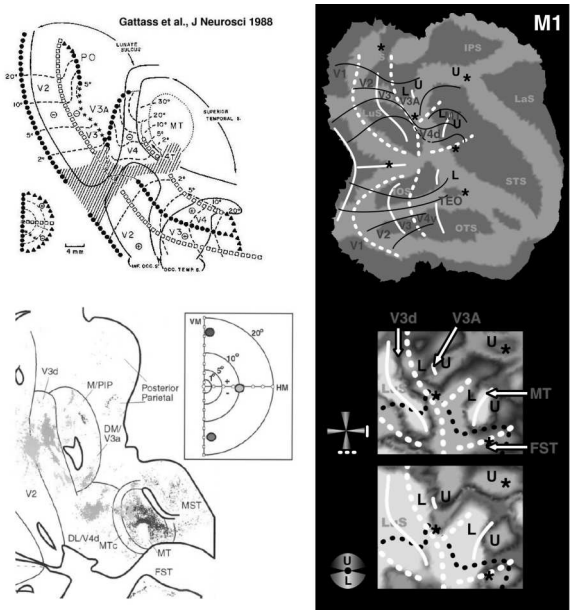

Figure 7. Comparison between our fMRI and previous electrophysiological results and connections patterns

A. Figure from Gattass et al 1988 (reproduced with permission). The results from this electrophysiological retinotopic mapping experiment shows a similar pattern of iso-eccentricity lines as observed in the present study (see iso-eccentricity lines in panel C) **B** Figure showing projections of VM and HM in V3A, V4 and MT/V5, extracted from Lyon and Kaas 2002 (reproduced with permission). **C** iso-eccentricity lines in right hemisphere of M1 derived from Fig. 5. **D** Close-up view of the horizontal and vertical meridians, upper and lower visual field representations around dorsal V4 (M1).

ACKNOWLEDGEMENTS

This work was supported by grants of the Queen Elisabeth Foundation (GSKE), the National Research Council of Belgium (NFWO; NFWO G0112.00), the Flemish Regional Ministry of Education (GOA 2000/11), the IUAP 4/22 and 5/11, Mapawamo (EU Life Sciences) and HFSP grant (RGY 14/2002). The authors thank M. De Paep, W. Depuydt, A. Coeman, C. Fransen, P. Kayenberg, G. Meulemans, Y. Celis, and G. Vanparrys for technical support. WV is a fellow of FWO-Flanders. We thank the Society for Neuroscience and Cell Press and the authors for the reproductions of Gattass et al. (1988) and Lyon and Kaas (2002) figures.

We thank Gilles Kahn, the Scientific Director of INRIA, for his warm support of our endeavour to explore the applications of computer science and mathematics to neurosciences.

Unité de Recherche INRIA Sophia Antipolis
2004, route des Lucioles - B.P. 93 - 06902 Sophia Antipolis Cedex (France)

Unité de Recherche INRIA Lorraine : Technopôle de Nancy-Brabois - Campus scientifique
615, rue du Jardin Botanique - B.P. 101 -54602 Villers lès Nancy Cedex (France)
Unité de Recherche INRIA Rennes : IRISA, Campus universitaire de Beaulieu - 35042 Rennes Cedex (France)
Unité de Recherche INRIA Rhône-Alpes : 655, avenue de l'Europe - 38330 Montbonnot St Martin (France)
Unité de Recherche INRIA Rocquencourt : Domaine Voluceau - Rocquencourt - BP 105 - 78153 Le Chesnay Cedex (France)

Editeur
INRIA - Domaine de Voluceau - Rocquencourt, B.P. 105 - 78153 Le Chesnay Cedex (France)
http:// www.inria.fr
ISSN 0249-6399